25th ABCM International Congress of Mechanical Engineering
October 20-25, 2019, Uberlândia, MG, Brazil

COB-2019-1074
PHENOMENOLOGICAL ASPECTS REGARDING THE AIR FLOW PAST A AHMED BODY WHEN MODELLING THE GROUND VELOCITY

Leonardo Mendes de Souza
Augusto Salomão Bornschlegell
UFGD, FAEN Rodovia Dourados - Itahum, Km 12 - Cidade Universitaria, Cx. Postal 364 - CEP 79804-970
leonardomendes3@hotmail.com, augustosalomao@ufgd.edu.br

Abstract. *The objective of the present study is to evaluate the ground's velocity boundary condition modelling of the flow around the Ahmed body. The ground is usually modeled as static, in spite of the fact that there is a relative velocity between the ground and the Ahmed body. The influence of this boundary condition is evaluated using the CFD tool OpenFOAM 6.0. Phenomenological aspects are pointed out such as the behavior of the stagnation point, recirculation zones and aerodynamic forces. The later demosntrated to be underestimated if unappropriated boundary conditios are applied.*

Keywords: *Ahmed body, CFD, fluid flow modelling.*

1. INTRODUCTION

The use of numerical tools to simulate engineering problems has become a commom practice since one can easily test different setups and different engineering scenarios without building a prototype. This easyness, combined with friendly user interface and a computer can lead to pitfalls if the modelling does not represent the studied phenomena.

Modelling requires some premisses to be considered. According to the evaluated enginnering problem, it is assumed a (simplified) geometry, some physical properties values, boundary conditions and the related equations set to be solved.

Fluid flow numerical modelling relies, of course, on the preavious parameters and on particular parameters, such as the relation between the domain discretization refinement and the numerical treatment for the Navier-Stokes advective terms, the pressure-velocity coupling strategy for quasi-permanent and transient flows, mesh sensibility and the relation between near wall discretization and turbulence modelling.

The most studied model for the flow around ground vehicles - the Ahmed body (Fig. 1) - was proposed by Ahmed *et al.* (1984). By means of a simplified geometry, different flow characteristics are exploited, such as drag and lift coefficients, flow detachment and reattachment, recirculating zones and vortex shedding patterns. The most studied variable in such flows is the slant angle α on the rear part of the body.

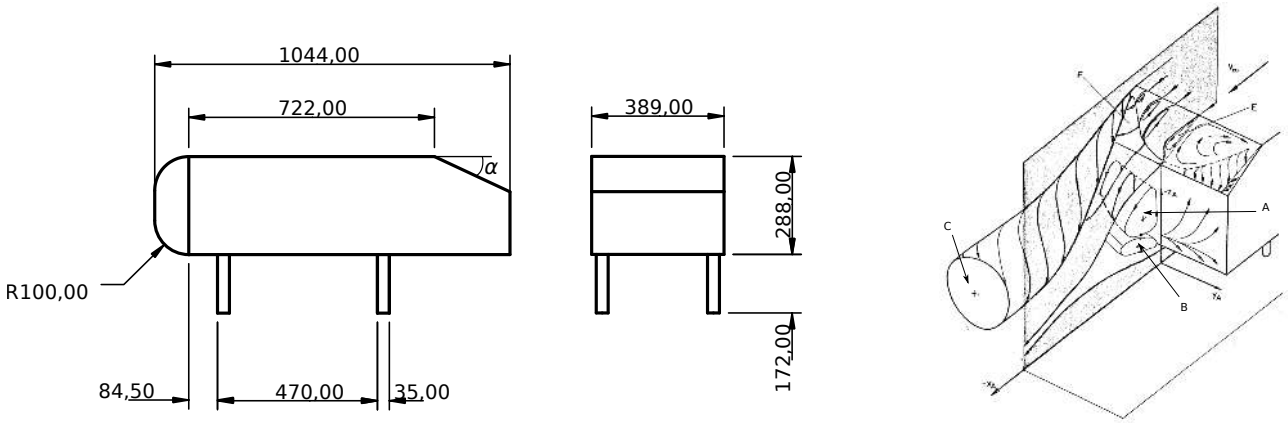

Figure 1. Flow patterns for $\alpha = 30°$. Adapted from Ahmed *et al.* (1984)

Regarding the ground velocity modelling, few works are observed. A comparative numerical work is presented by (Krajnović and Davidson, 2005). The authors discuss the challenges related to the experimental setup that provides relative velocity between the Ahmed body and the ground. The major concern is how to fix the Ahmed body, since the moving

ground does not offer mechanical support. According to their research, drag and lift decrease by 8 and 16 %, respectively, when the ground relative velocity is considered.

In the present work, attention is given to the flow region between the Ahmed body and the ground. Since it is much easier to run experiments with a stationary ground setup, most works do not take its relative motion into account. This information is a boundary condition; a basic parameter to be evaluated regardeless of the employed metodology (i.e. numerical, experimental or analytical). Thus, the present work presents a comparison between static and moving wall (ground) boundary conditions in the Ahmed flow modelling.

2. LITERATURE REVIEW

Ahmed *et al.* (1984) identified 4 main vortex structures (Fig. 1). Regions A, B and D are the recirculation zones formed behind the Ahmed bluffy body. The C region is the result of the flow interaction that just detached the body's surface and the recirculating regions in the near wake.

The slant angle α imposes the wake behavior and consequently has influence on the drag and lift coefficients. According to Hanfeng *et al.* (2016), 3 distinct slant angle flow groups are identified. The first, for $\alpha \leq 12.5°$, the fluid flow develloped on the top body's surface follows the slant surface without any flow separation. The drag coefficient (C_d) virtually does not change with α. For $12.5° < \alpha < 30°$, the structures become three-dimensional and it is observed the detachment and reattachment of the flow on the slant surface. This new recirculating zone increases the C_d, which has its maximum value for α 30. When $\alpha > 30°$, the flow on the slant surface is not able to reattach anymore. A constant pressure distribution on the near wake is observed with a considerable drop in the C_d value. The authors studied the influence of different deflectors geometries at the edge which intersects the top surface and the slant angled rear surface.

Different numerical models were compared with experimental data in order to evaluate the Ahmed flow. Guilmineau *et al.* (2018) employed two hybrid RANS-LES (Reynolds Averaged Navier-Stokes - Large Eddy Simulation) formulations: the DES (Detached Eddy Simulation) and the IDDES (Improved Delay Detached Eddy Simulation). The later provided good agreement with experimental data. Pure LES models were tested and compared with experimental data by Tunay *et al.* (2016), Krajnović and Davidson (2005), Krajnović *et al.* (2012) and Serre *et al.* (2013). Corallo *et al.* (2015) employed the k-ω SST (Menter, 1994) turbulence model.

Table 1 presents a non-exaustive list of different studies dedicated to study the Ahmed body. The Reynolds Number (Re), based on the vehicle's height, stands between 10^3 and 10^6.

Table 1. Typical Reynolds Numbers in numerical and experimental works concerning the flow past the Ahmed body.

Author	Study	Re
Ahmed *et al.* (1984)	Experimental	$4.29\ 10^6$
Mathey and Cokljat (2005)	Numerical	$7.68\ 10^5$
Fares (2006)	Numerical	$1\ 10^6$
Bruneau *et al.* (2007)	Numerical	$8.275\ 10^3$
Thacker *et al.* (2012)	Experimental	$1\ 10^6$
Kourta and Leclerc (2013)	Experimental	$1.2\ 10^6$
Gulyás *et al.* (2013)	Experimental	$2\ 10^5$
Mirzaei *et al.* (2015)	Numerical	$3\ 10^4$ - $3\ 10^5$
Hanfeng *et al.* (2016)	Experimental	$8.7\ 10^5$
Meile *et al.* (2016)	Experimental	$2.78\ 10^6$
Tunay *et al.* (2016)	Both	$1.48\ 10^4$
Raina *et al.* (2017)	Numerical	$3.1\ 10^5$ - $7.7\ 10^5$
Guilmineau *et al.* (2018)	Numerical	$7.68\ 10^5$
Rao *et al.* (2018)	Both	$2\ 10^6$
Present work	Numerical	$1.65\ 10^4$ - $8.28\ 10^4$

It is worth mentioning other geometries than the Ahmed body in ground vehicles aerodynamics. Östh and Krajnović (2014) evaluated the aerodynamics of a generic container freight wagon numerical model. A full real 25-ton truck geometrical model was evaluated by Nakashima *et al.* (2013), considering, in addition to the foward movement, a crosswind flow. Independently of the geometry, the present work drawns attention to the fact that the relative ground velocity shall not be neglected in ground vehicles aerodynamics.

3. NUMERICAL MODEL

The air flow past the Ahmed body was modelled as two-dimensional, isothermal, transient and with constant properties. The numerical tool employed was the OpenFOAM 6.0, the pisoFoam solver. The domain, mesh and boundary

conditions are presented in Fig. 2. The geometry's slant angle is 25°. The Ahmed body is positioned about 10 times its height from the inlet and top surfaces. This domain setup was based on preavious works, such as (Krajnović and Davidson, 2005) and (Guilmineau *et al.*, 2018). The final mesh, created with the snappyHexMesh utility, is composed by 160 k hexahedral elements. The snappyHexMesh tool creates tridimensional meshes. In order to create a 2D (lighter) model with only one volume in the plane perpendicular direcion, the initial 3D frontal patch was extruded. Layers are employed to control the y+ value. The turbulence model employed was the Spalart Allmaras (P. R. Spalart, 1992), so the mesh refinement was set to ensure y+ lesser than 1. Mesh sensibility analysis was also performed by increasing in two times the number of elements in each model direction (x, y) in the blockMesh utility. This strategy led to a 260 k hexahedral element mesh. The difference in the aerodynamic forces obtained in the finner mesh is less than 0.2 %.

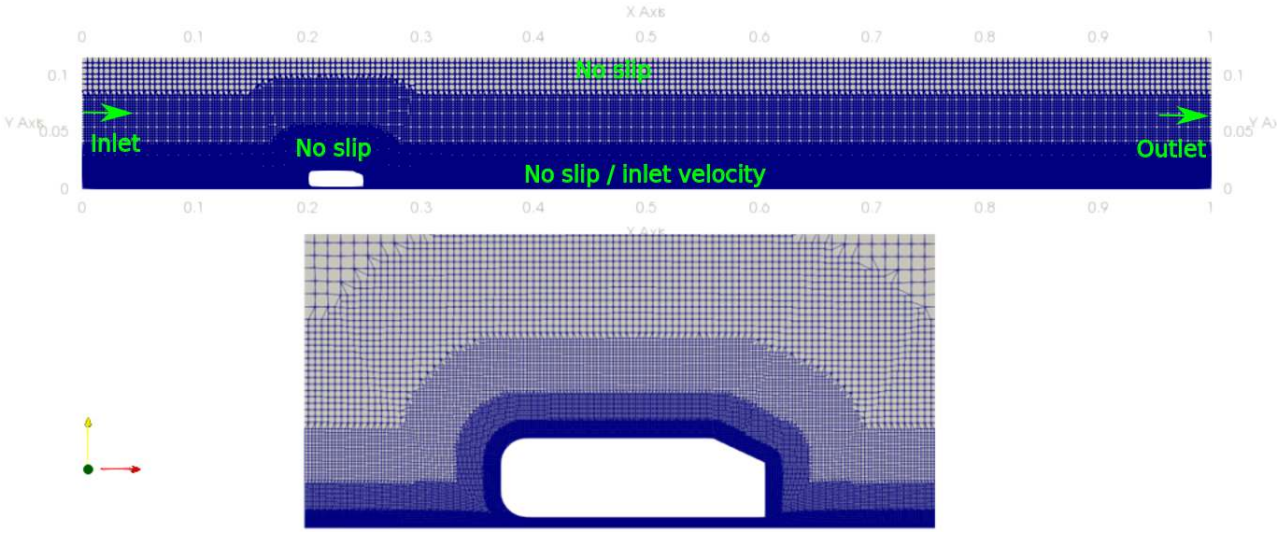

Figure 2. Mesh and boundary conditions

The initial flow velociy field corresponds to the inlet velocity. The total physical time simulated is 1 second. As boundary conditions, it was imposed an uniform inlet velocity at the inlet; symetry (no slip) at the top boundary and the inlet/outlet boundary condition at the outlet. At the ground, static and moving ground at different inlet velocities were evaluated. At the Ahmed body, it was imposed the static (no-slip) boundary condition.

The governing parameter in this model - the Reynolds Number - is defined in Eq. (1):

$$Re = \frac{\rho V L}{\mu} \tag{1}$$

where ρ stands for the air density [kg.m^{-3}], V represents the free stream velocity [m.s^{-1}], L represents the Ahmed's body height [m] and μ stands for the air viscosity [Pa.s].

Three inlet velocities, and then, three Reynolds Numbers (cases) were evaluated: Re_A =1.65 10^4 (10 m.s^{-1}), Re_B =3.31 10^4 (20 m.s^{-1}) and Re_C =8.28 10^4 (50 m.s^{-1}). For all cases, the inlet turbulent intensity was set to 5 %.

The temporal discretization was set to ensure the Courant Number lesser than 1 and solved usind the second order backward scheme. The employed discretization schemes for the Navier-Stokes difusive and advective terms were Gauss linear and linear upwind, respectivelly. PisoFoam solver uses the PISO algorithm for the pressure-velocity coupling. The relaxation factors for pressure and velocities were set to 0.3 and 0.7, respectivelly.

4. RESULTS AND DISCUSSION

The velocity and pressure fields are presented for all the three cases studied in the present work (Fig. 3, 4 and 5) for the time of 1 s. No noticable change in the flow fields were observed along the simulated time, so that the flow behavior is quasi-static. The absence of vortex shedding from the Ahmed body implies null Strouhal Number, reconfirming its quasi-static behavior. When imposing the inlet velocity to the ground boundary condition, more fluid flows through the gap between the Ahmed body and the ground. As a consequence, the recirculation region in front of the Ahmed body vanishes, pulling the stagnation point downwards. The recirculation in front of the Ahmed body creates a deviation of the fluid flow, so that, when flow passes by the upper edge of the Ahmed body and detaches, a smaller recircualtion zone is observed on the top surface. That is why reattachment in this case occurs sooner. The flow detaches at the edge formed by the intersection of the top surface and the slant surface. No reattachment is observed in the slant surface. The recirculation zone behind the Ahmed body in both cases are alike; the most different behavior observed is in the frontal region.

Regarding the pressure fields, it is observed on the Ahmed body top surface that, the low level pressures, for the moving ground boundary condition cases, extends to a broader area. That behavior, associated with the stagnation point displacement downwards, implies in higher lift coefficients for all cases (Fig. 9). At the rear wake, the pressure magnitude is slightly lower for the moving ground cases. This fact combined with the absence of the uptream recirculating zone led to an increase of the drag coefficient. The increase in both aerodynamic forces is consistent with the ploted velocity and pressure fields, although Krajnović and Davidson (2005) noticed the oposite behavior in their tridimensional model. Indeed, in their model, the most expressive diferences occur close to the slant surface, fact not identified in the present model.

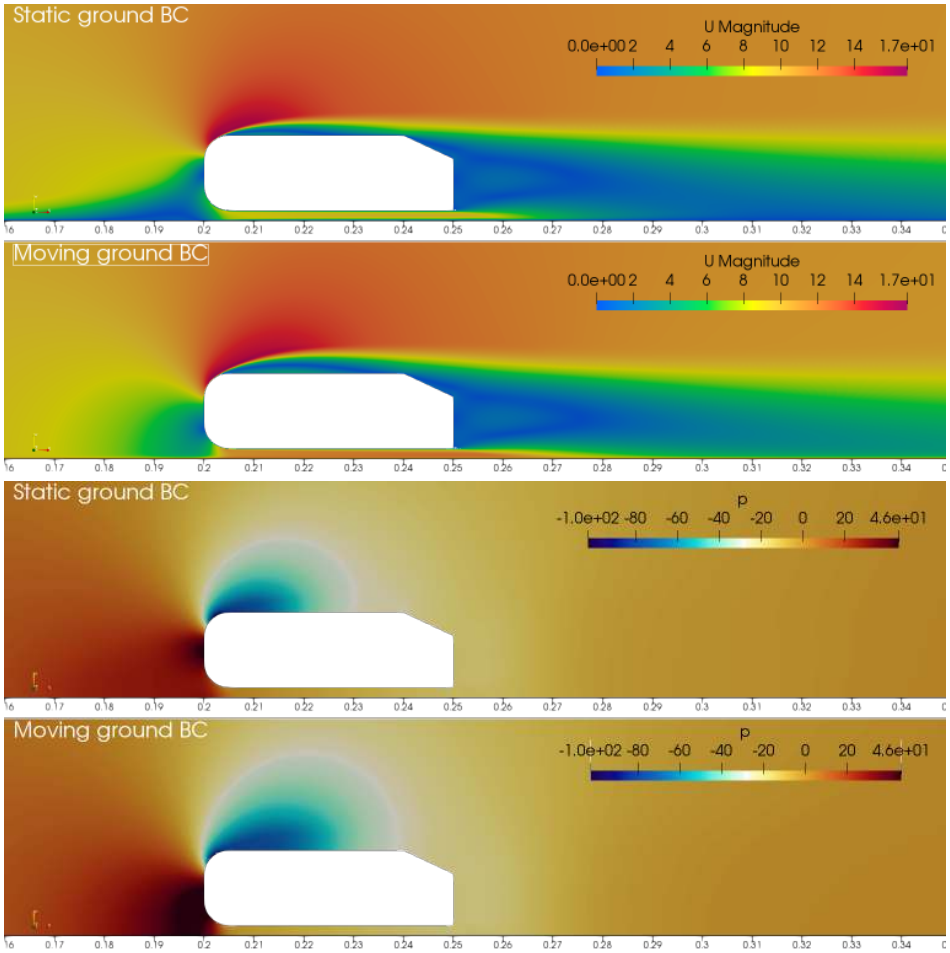

Figure 3. Case A: Re_A =1.65 10^4 (10 m.s^{-1}). Velocity in m.s^{-1} and Pressure in Pa

The velocity profiles along the domain are presented in Fig. 6, 7 and 8 for the imposed velocities of 10, 20 and 50 m.s^{-1} respectively. For the positions in the x axis between 0.17 and 0.19 m, the velocity profiles have constant values in the height interval between 0.07 and 0.12 m. Its value decreases gradually from 10 m.s^{-1} to 8 m.s^{-1} (V = 10 m.s^{-1}), from 22 to 17 m.s^{-1} (V = 20 m.s^{-1}) and from 53 to 43 m.s^{-1} (V = 50 m.s^{-1}).

For x = 0.20, there is the Ahmed body frontal face. The Ahmed body's blockage induces the flow acceleration, due continuity. This accelaration, at height = 0.03 m, promotes an inflexional velocity profile, which was kept stable downstream for all the studied Reynolds Numbers. For the heights between 0.01 and 0.03, the velocity profile decelerates from its maximum value to zero, since it is the Ahmed body frontal face position. The region between the ground and the Ahmed body presents new accelaration profile.

At the position x = 0.25 m, there is the Ahmed body rear face. Then, in the interval between 0.20 < x < 0.25, the inflexional velocity profile is maintained. The highest velocity magnitude is between x = 0.20 and x = 0.21 m. For V = 10 m.s^{-1}, 0.20 < x < 0.25 m and 0.015 < height < 0.020, reverse flow is obseved in both frontal and slant surface regions. As inertial forces increases with the increasing inlet velocity, reverse flow tends to occur only at the slant face region.

The velocity profiles loose their inflexion point from x > 0.30 m on. As the profiles devellop along the x axis, they tend to become uniform.

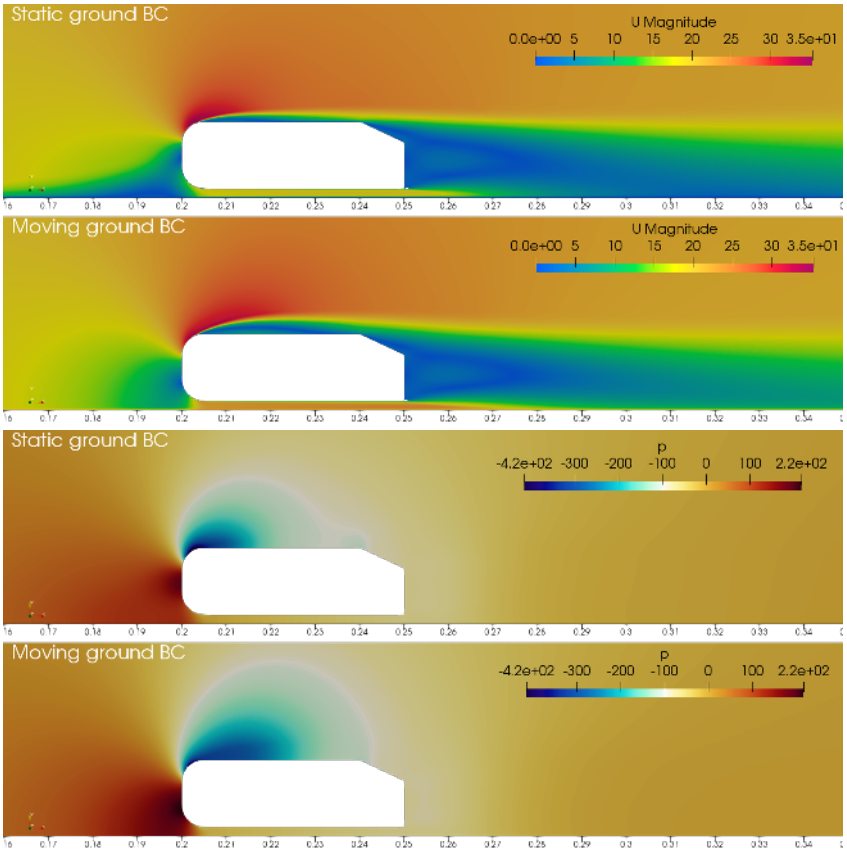

Figure 4. Case B: Re_B =3.31 10^4 (20 m.s^{-1}. Velocity in m.s^{-1} and Pressure in Pa

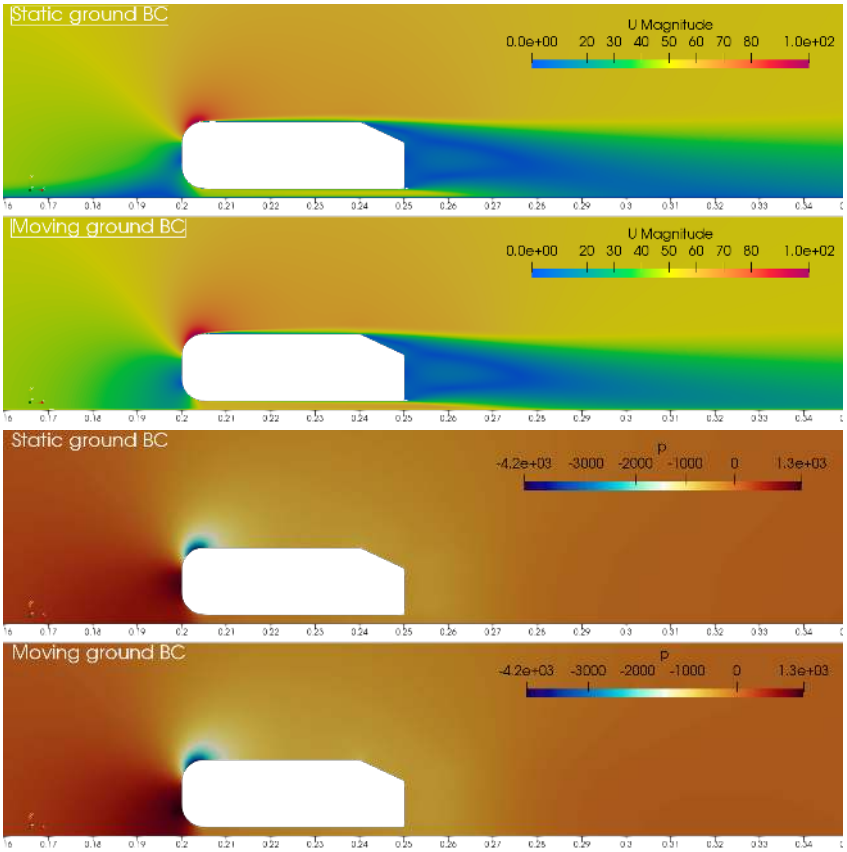

Figure 5. Case A: Re_C =8.28 10^4 (50 m.s^{-1}). Velocity in m.s^{-1} and Pressure in Pa

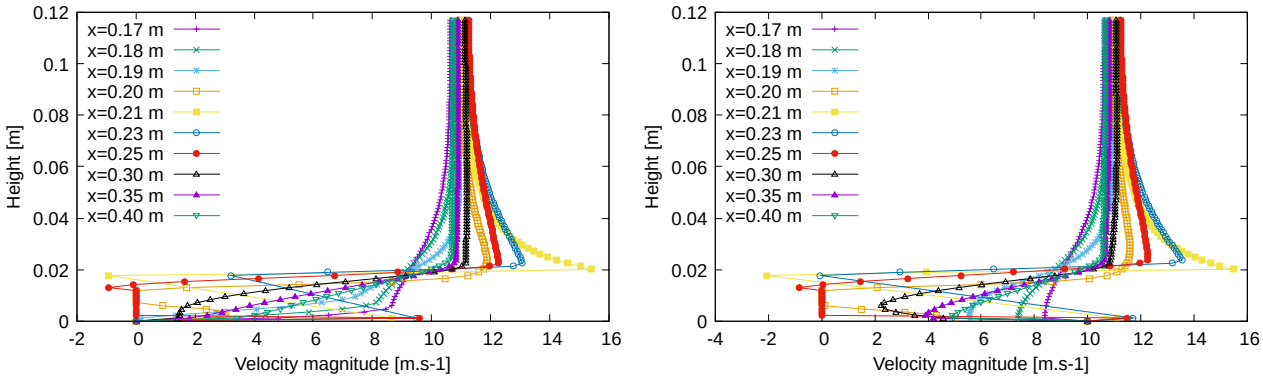

Figure 6. Velocity profiles for Re_A =1.65 10^4 (10 m.s^{-1}); static ground (left) and moving ground (right)

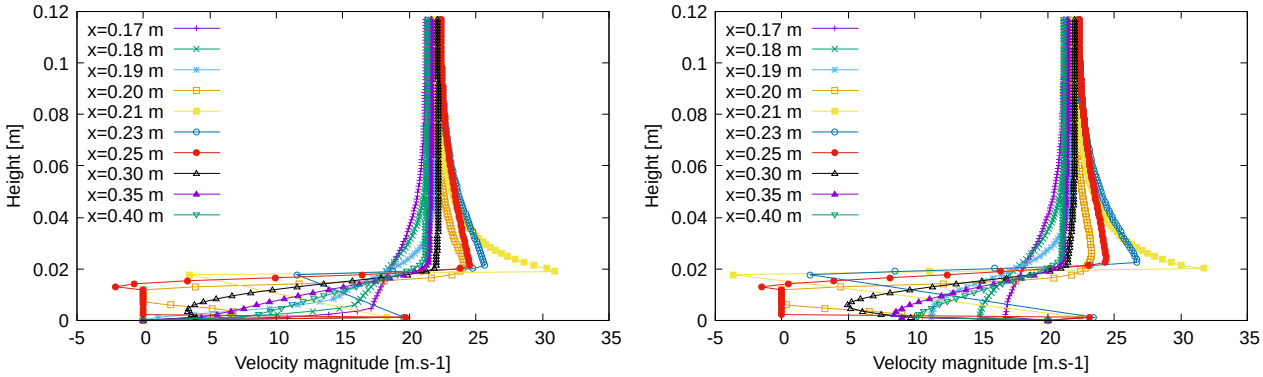

Figure 7. Velocity profiles for Re_B =3.31 10^4 (20 m.s^{-1}); static ground (left) and moving ground (right)

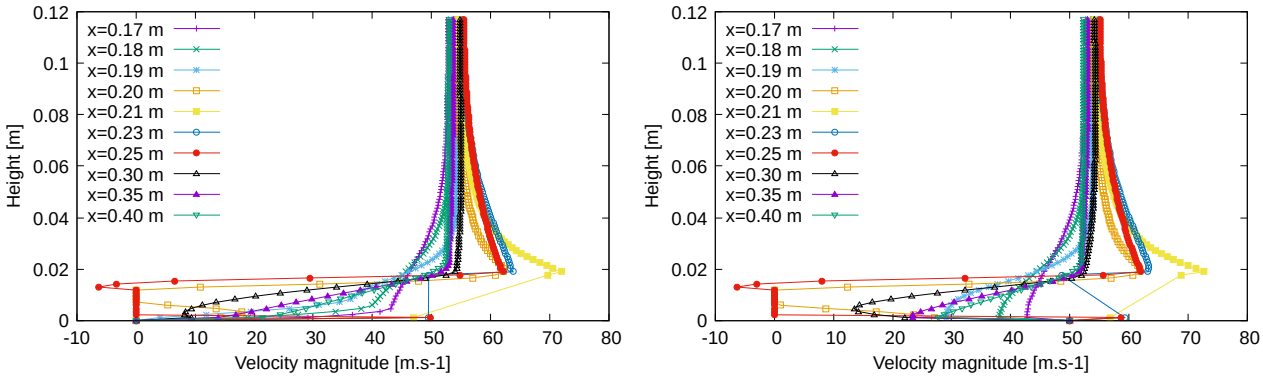

Figure 8. Velocity profiles for Re_C =8.28 10^4 (50 m.s^{-1}); static ground (left) and moving ground (right)

For the drag (CD) and lift (CL) coefficients evaluation, it is considered a width of 0.020 m; keeping the aspect ratio of the original Ahmed work. As pointed out earlier, in Fig. 9, it can be verified that all the aerodynamic forces related to the moving boundary condition are greater than the corresponding static cases. For Re_A =1.65 10^4 (10 m.s^{-1}), CL increased in 10 % and CD in 15.6 %. For Re_B =3.31 10^4 (20 m.s^{-1}), CL increased in 14.7 % and CD in 16.7 %. This was the most significative difference between models. For Re_C =8.28 10^4 (50 m.s^{-1}), CL increased in 3 % and CD in 6.7 %.

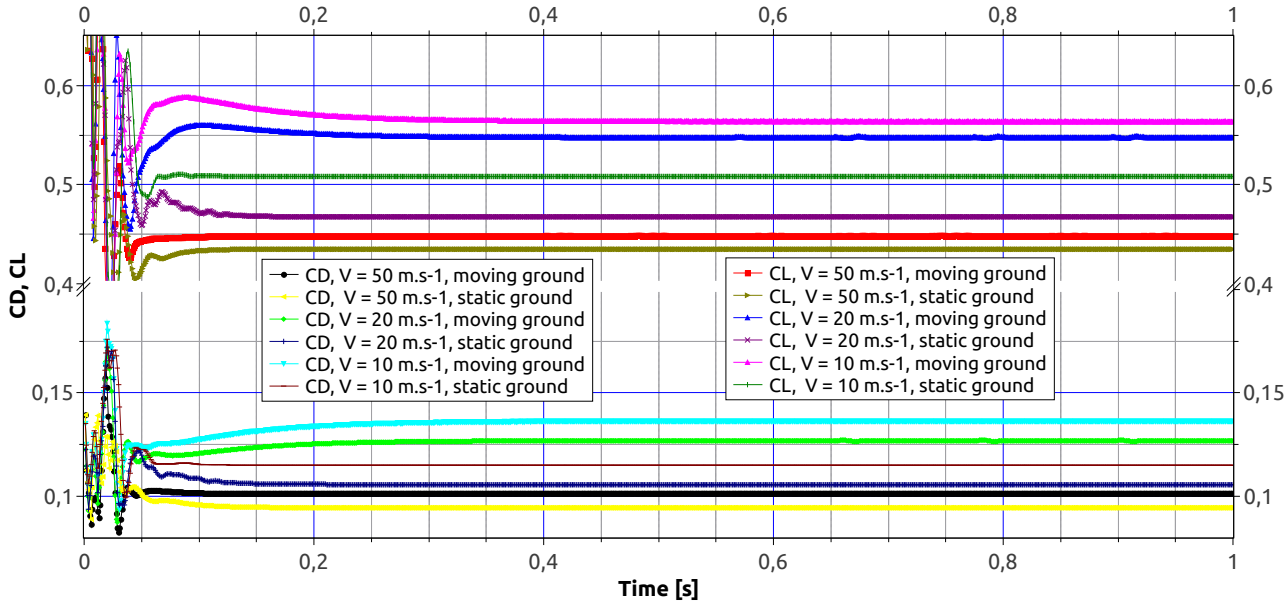

Figure 9. Drag (CD) and lift (CL) coefficients

5. CONCLUSION

In this work, the ground boundary condition effect on the Ahmed flow was numerically evaluated. The flow dynamics demonstrated to behave differently when the relative ground velocity is considered. The most perceptible differences identified were on the frontal region of the Ahmed body, such as the recirculation zone supression and the displacement of the stagnation point downwards. Differences in the aerodynamic forces attained up to 16.7 %. Then, the ground imposed velocity shall be considered in ground vehicle aerodynamic studies.

6. ACKNOWLEDGEMENTS

The authors present their ackknowledgements to the University of Grande Dourados - UFGD - for its support during the devellopment of the present work.

7. REFERENCES

Ahmed, S.R., Ramm, G. and Faltin, G., 1984. "Some Salient Features Of The Time-Averaged Ground Vehicle Wake". *SAE Technical Paper 840300*.

Bruneau, C.H., Gilliéron, P. and Mortazavi, I., 2007. "Flow manipulation around the ahmed body with a rear window using passive strategies". *Comptes Rendus Mécanique*, Vol. 335, No. 4, pp. 213 – 218.

Corallo, M., Sheridan, J. and Thompson, M., 2015. "Effect of aspect ratio on the near-wake flow structure of an ahmed body". *Journal of Wind Engineering and Industrial Aerodynamics*, Vol. 147, pp. 95 – 103.

Fares, E., 2006. "Unsteady flow simulation of the ahmed reference body using a lattice boltzmann approach". *Computers & Fluids*, Vol. 35, No. 8, pp. 940 – 950.

Guilmineau, E., Deng, G., Leroyer, A., Queutey, P., Visonneau, M. and Wackers, J., 2018. "Assessment of hybrid rans-les formulations for flow simulation around the ahmed body". *Computers & Fluids*, Vol. 176, pp. 302 – 319.

Gulyás, A., Bodor, Á., Regert, T. and Jánosi, I.M., 2013. "Piv measurement of the flow past a generic car body with wheels at les applicable reynolds number". *International Journal of Heat and Fluid Flow*, Vol. 43, pp. 220 – 232. ISSN 0142-727X. 7th International Symposium on Turbulence Heat & Mass Transfer (THMT-7), Palermo Conference on Modelling Fluid Flow (CMFF 12).

Hanfeng, W., Yu, Z., Chao, Z. and Xuhui, H., 2016. "Aerodynamic drag reduction of an Ahmed body based on deflectors". *J. Wind Eng. Ind. Aerodyn.*, Vol. 148, pp. 34–44.

Kourta, A. and Leclerc, C., 2013. "Characterization of synthetic jet actuation with application to ahmed body wake". *Sensors and Actuators A: Physical*, Vol. 192, pp. 13 – 26.

Krajnović, S., Ringqvist, P., Nakade, K. and Basara, B., 2012. "Large eddy simulation of the flow around a simplified train moving through a crosswind flow". *Journal of Wind Engineering and Industrial Aerodynamics*, Vol. 110, pp. 86 – 99.

Krajnović, S. and Davidson, L., 2005. "Influence of floor motions in wind tunnels on the aerodynamics of road vehicles".

J. Wind Eng. Ind. Aerodyn., Vol. 93, No. 9, pp. 677–696.

Mathey, F. and Cokljat, D., 2005. "Zonal multi-domain rans/les simulation of airflow over the ahmed body". In W. Rodi and M. Mulas, eds., *Engineering Turbulence Modelling and Experiments 6*, Elsevier Science B.V., Amsterdam, pp. 647 – 656.

Meile, W., Ladinek, T., Brenn, G., Reppenhagen, A. and Fuchs, A., 2016. "Non-symmetric bi-stable flow around the ahmed body". *International Journal of Heat and Fluid Flow*, Vol. 57, pp. 34 – 47.

Menter, F.R., 1994. "Two-equation eddy-viscosity turbulence models for engineering applications". *AIAA Journal*, Vol. 32, No. 8, pp. 1598–1605.

Mirzaei, M., Krajnović, S. and Basara, B., 2015. "Partially-averaged navier-stokes simulations of flows around two different ahmed bodies". *Computers & Fluids*, Vol. 117, pp. 273 – 286.

Nakashima, T., Tsubokura, M., Vázquez, M., Owen, H. and Doi, Y., 2013. "Coupled analysis of unsteady aerodynamics and vehicle motion of a road vehicle in windy conditions". *Computers & Fluids*, Vol. 80, pp. 1 – 9. Selected contributions of the 23rd International Conference on Parallel Fluid Dynamics ParCFD2011.

Östh, J. and Krajnović, S., 2014. "A study of the aerodynamics of a generic container freight wagon using large-eddy simulation". *Journal of Fluids and Structures*, Vol. 44, pp. 31 – 51.

P. R. Spalart, S.R.A., 1992. "A one-equation turbulence model for aerodynamic flows". *30th Aerospace Sciences Meeting and Exhibit*.

Raina, A., Harmain, G. and Haq, M.I.U., 2017. "Numerical investigation of flow around a 3d bluff body using deflector plate". *International Journal of Mechanical Sciences*, Vol. 131-132, pp. 701 – 711.

Rao, A., Minelli, G., Basara, B. and Krajnović, S., 2018. "On the two flow states in the wake of a hatchback ahmed body". *Journal of Wind Engineering and Industrial Aerodynamics*, Vol. 173, pp. 262 – 278.

Serre, E., Minguez, M., Pasquetti, R., Guilmineau, E., Deng, G.B., Kornhaas, M., Schäfer, M., Fröhlich, J., Hinterberger, C. and Rodi, W., 2013. "On simulating the turbulent flow around the ahmed body: A french-german collaborative evaluation of les and des". *Computers & Fluids*, Vol. 78, pp. 10 – 23.

Thacker, A., Aubrun, S., Leroy, A. and Devinant, P., 2012. "Effects of suppressing the 3d separation on the rear slant on the flow structures around an ahmed body". *Journal of Wind Engineering and Industrial Aerodynamics*, Vol. 107-108, pp. 237 – 243.

Tunay, T., Yaniktepe, B. and Sahin, B., 2016. "Computational and experimental investigations of the vortical flow structures in the near wake region downstream of the ahmed vehicle model". *Journal of Wind Engineering and Industrial Aerodynamics*, Vol. 159, pp. 48 – 64.

8. RESPONSIBILITY NOTICE

The authors are the only responsible for the printed material included in this paper.